

# Relation of OSNR and PLR for nonintrusive fault detection in all-optical IP–Ethernet–WDM networks

Carolina Pinart

*Centre Tecnològic de Telecomunicacions de Catalunya, Avenue Canal Olímpic s/n  
08860, Castelldefels, Barcelona, Spain  
e-mail: carolina.pinart@cttc.cat*

Received November 27, 2007; revised February 1, 2008;  
accepted February 2, 2008; published March 7, 2008 (Doc. ID 90077)

I present an analytical expression for the relation of the packet loss rate (PLR) with respect to the channel optical signal-to-noise ratio measured nonintrusively in an all-optical, wavelength-routed network. This closed-form expression is aimed for rapid, nonintrusive fault detection of lambda services. This relation will help achieve reliable all-optical networks with no extra optoelectrical cost due to monitoring, and yet have digital parameters such as the PLR in the service level agreements. Analytical results considering performance thresholds for triple-play services, gigabit Ethernet framing, and forward error correction are discussed. © 2008 Optical Society of America

*OCIS codes:* 060.1155, 060.2330, 060.4250, 060.4253, 060.4257, 060.4265.

## 1. Introduction

Today's optical networks are composed of amplified fiber segments in which digitized data are transported analogically and electrical equipment based on the synchronous digital hierarchy (SDH) architecture [1]. An all-optical or transparent optical network is composed of amplified fiber segments and photonic equipment. This means that data travel from the source node to the destination node without undergoing optoelectrical (OE) conversions. The advantages of this architecture are well-known and include high bandwidth, especially when using wavelength division multiplexing (WDM), and independence of the bit rate and format of the data transported.

However, the absence of electrical regeneration in all-optical networks results in fault propagation, that is, in the generation of multiple alarms for a single failure. This propagation, which occurs downstream on all affected light paths from the origin of the fault, increases the complexity of fault localization. Transparency also limits the amount of performance parameters available in the core nodes, which are fully analog (optical). On the other hand, the huge amount of information transported in optical networks makes rapid fault localization a must to cope with service quality, which results in bounded unavailability times. For example, with SDH's automatic protection switching, services are to be disrupted less than 50 ms.

Fault management is a crucial aspect in deploying any network architecture. Regardless of the network type, a service level agreement (SLA) always includes survivability aspects in the form of service availability (e.g., the five 9s) or mean time to repair, among others. Indirectly, the most important quality parameter in a SLA, the bit error rate (BER), also reports on the reliability of the network, since it indicates the goodness of information transport over the network. Fault management is based on detecting and localizing faults and failures. Fault localization mechanisms are usually based on alarms generated by different types of network monitoring equipment that measure performance parameters of different layers of the Open Systems Interconnection (OSI) architectural model. In turn, the nature and amount of these alarms depend on the placement and capabilities of the monitors. In SDH systems, the information on signal quality is analogically monitored at the physical layer through optical input and output power monitoring and is digitally monitored at the physical and data link layers through bit interleaved parity error counting and frame synchronization, respectively [2].

Applying the digital supervising methodologies of SDH to wavelength-routed all-optical networks is infeasible from the viewpoint of alarm detection and fault localization, as demonstrated in [3], because all-optical cross-connect-type systems cannot employ bit-oriented data transmission even with extensive modification. Only edge nodes—destination of light paths, where OE conversions take place—can have direct access to the digital data. For this reason, fault detection and localization in all-optical networks is an open research topic that encompasses detection models and methods, the selection of performance parameters to cover the maximum range of faults while ensuring cost-effectiveness and maintaining transparency, the placement of monitoring equipment to reduce the number of redundant alarms and to lower the capital expenses, and the design of fast localization algorithms.

In the context of fault detection, this work presents an analytical relation between two performance parameters that can be easily obtained without converting a WDM signal into a digital one, i.e., which can be obtained nonintrusively. These two parameters are the optical signal-to-noise ratio (OSNR), which can be obtained anywhere in the all-optical network by tapping the fiber links, and the packet loss rate (PLR), which can be measured at the ingress–egress of light paths (IP routers). The OSNR can be related with the BER, which is commonly used for fault detection, while the PLR is one of the major packet metrics in IP-related SLAs. Within the context of IP–Ethernet over WDM networks, both the OSNR and the PLR are expected to become basic performance parameters for fault detection.

The remainder of the paper is organized as follows. Section 2 provides an overview of fault detection and localization in all-optical networks. In Section 3 I describe the proposed relation between the OSNR and the PLR in intensity-modulation, direct-detection, all-optical networks enabled with forward error correction (FEC) and gigabit Ethernet framing. Section 4 discusses the numerical results obtained and shows the graphical OSNR–PLR relation for triple-play lambda services carried over an IP–Ethernet–WDM all-optical network. Finally, in Section 5 I draw conclusions.

## 2. Fault Detection and Localization in All-Optical Networks

Fault localization finds the minimum set of potential failed network resources based on the alarms generated during fault detection. The basis for fault detection is the monitor, which is an entity that surveys the operating condition of a network element. Monitors are usually embedded with the capability of reporting fault conditions to external entities, known as fault management systems. The identification and location of failures in all-optical networks is complex due to three main issues:

- **Fault propagation.** Due to transparency, a single failure may trigger a large number of alarms, which results in redundancy and/or false alarms. Table 1 illustrates the alarms raised at different layers of an all-optical network for a single failure.
- **Limited availability of digital information.** The supervisory information located in the overhead and/or payload of the data (e.g., data link and network layers in Table 1) can only be processed at the source or destination of an optical connection, where the OE conversions take place. The physical-layer performance parameters can be digital or analog. In the digital domain, we find the BER and the signal-to-noise ratio (SNR). There are several analog parameters that can be obtained in an optical network; in this work, I focus on the channel OSNR. From the physical layer up, all the performance parameters are digital. The most important data-link-layer parameter is the block or frame error rate, depending on the layer-two technology (e.g., Ethernet). The most important network-layer parameters are the PLR, the packet delay,

**Table 1. Generation of Alarms for a Single Failure**

OSI Layer	Fiber Cut (Power Loss)	D/mux Malfunction (Cross Talk)
Physical (O)	Loss of light	OSNR decrease
Physical (E)	—	BER increase
Data link	Frame loss	Increase in block errors
Network	Loss of connectivity	Packet error rate increase

**Table 2. Fault Localization Mechanisms in the Literature**

Approach	Based On	Name	Reference
Centralized	Model of optical elements' behavior, uses alarm filtering	Transparent failure location algorithm	[7]
	Model of physical topology	Inference algorithm	[8]
	Probabilistic failure model	Run-length probing algorithm	[9]
	Monitoring cycles	Heuristic spanning tree with $m$ -cycle	[10]
Distributed	Notification of the status of data channels in a link	Link management protocol	[11]
	Keep alive packets along the established light path	End-to-end hello fault detection and localization protocol	[12]

and the jitter. Of course, translating the SLA parameters into an optical connection only makes sense if a single service—from one to several users, but all with the same service class—is carried on a WDM channel, i.e., a lambda service.

- **Limited processing time.** Due to the bounded delay for triggering protection–restoration actions imposed by SLAs, fault localization must be rapid. However, the problem of locating multiple faults is nondeterministic-polynomial-time- (NP-) complete [4], which means that the processing time of a fault management system of a large meshed optical network may become an issue. Since the early 1990s, research efforts in managing multiple failures have been focused on reducing the number of monitors [5,6], placing monitoring equipment in optimal locations [6,7], and developing fast localization algorithms [8–12]. Table 2 illustrates the most representative centralized and distributed approaches for fault localization in all-optical networks.

### 3. Proposed Model for Fault Detection in All-Optical Networks

In general, fault detection involves the discovery of states or conditions not meeting desirable or expected objectives, such as a BER value or an exceeded OSNR threshold. When a fault is detected, a network element will often send a notification or alarm. This means that at any layer of the OSI stack, monitors provide measurements and/or raise threshold crossing alarms (TCAs) whenever a monitored performance parameter is under or above a preconfigured threshold.

In this work, the monitors perform nonintrusive monitoring of the status of data and resources in the network. Note that if we want to obtain performance information in an all-optical network without regenerating the optical signal, we are basically limited to spectral information (e.g., optical channel power or OSNR) in the core nodes and digital information after the photoreceiver, i.e., at the egress of the light path. Because of this lack of digital information in the core nodes, there is a need to relate spectral information to the digital information that is part of the SLA, namely, the BER and PLR. This is especially useful for early detection of faults in the core of the network that jeopardize the quality of service (QoS) guarantee, that is, to estimate the PLR of data when the signal starts to degrade (channel OSNR decreases).

#### 3.A. Framework and Assumptions

Figure 1 illustrates the network model considered in this paper, which was derived in

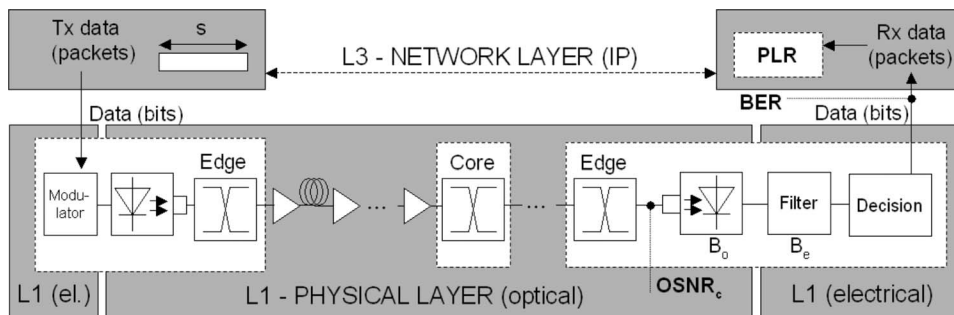


Fig. 1. Connection from a source to a destination (physical and network layers).

a previous work by the author [13]. The figure represents an arbitrary end-to-end path (light path) between a source and a destination node and shows that the sources of errors are only found in bit distortions at the optical path due to the addition of noise and to imperfections of network elements. The all-optical network carries IP packets, which are structured as an IP header followed by a variable-length data field. For simplicity, we consider that the average length of an IP packet  $L$  is expressed as

$$L = H + P, \tag{1}$$

where  $H$  is the length of the IP packet header (20 bytes for IPv4), and  $P$  denotes the average length of the data field. In IP over gigabit Ethernet (GigE) over WDM networks, IP packets are mapped directly into GigE. Due to this encapsulation, an overhead of  $H_{\text{GigE}}=272$  bits (34 bytes) is added per packet [14]. For example, a 512 byte IP packet ( $L=4096$  bits) encapsulated in GigE corresponds to 4368 bits.

After the GigE framing, we add the FEC encoding at the physical layer. In this work, I consider Reed–Solomon (RS), which is the most common FEC scheme. A RS code word of  $n$  bytes is composed of  $k$  bytes of data and  $2t$  bytes of parity, where  $t$  is the maximum number of symbol errors in the code word. Then, a RS (255,239) code has  $n=255$ ,  $k=239$ , and  $t=8$ , that is, up to 64 bits can be corrected (symbols are 8-bits long). This is the code recommended by the ITU-T for optical fiber submarine cable systems and is the most deployed scheme in FEC-enabled optical networks. For the previous example, applying RS (255,239) would lead to the transmission of 4660 bits per IP packet ( $\sim 7\%$  overhead). Figure 2 illustrates the receiver side for the schemes described above.

As defined in [15], we assume that there is a probability for a bit error in every bit (anywhere in the packet) and that bit errors are independently and identically distributed. Finally, we assume low intersymbol interference, Gaussian amplified spontaneous emission (ASE) noise distribution, and ASE noise dominance over the receiver shot and thermal noises [16].

**3.B. Relation between the OSNR and the PLR**

The probability for the misinterpretation of a bit value at the receiver’s decision circuit (Fig. 1) is given by the BER between two regenerative end points [15], which in this work are the source and destination of a light path, before the FEC (Fig. 2). The BER is defined as

$$\text{BER} = \frac{\text{errored bits}}{\text{transmitted bits}}. \tag{2}$$

In this work, I consider intensity-modulation, direct-detection systems, as depicted in Fig. 1. Using the results of [16,17], the relation between the BER of a WDM channel and the channel OSNR ( $\text{OSNR}_c$ ) measured at the photoreceiver can be approximated as

$$\text{BER}_{\text{preFEC}} = \frac{1}{2} \operatorname{erfc} \left( \sqrt{\frac{B_o}{2B_e} \frac{2\text{OSNR}_c}{4\text{OSNR}_c + 1} + 1} \right), \tag{3}$$

where  $B_o$  and  $B_e$  are the optical and electrical bandwidths of the receiver filter (Fig. 1). Note that  $\text{OSNR}_c$  is measured at the photoreceiver, that is, before the FEC, and hence the BER estimated using Eq. (3) is called  $\text{BER}_{\text{preFEC}}$ . In [18], Torrieri approximates the relation between the input ( $\text{BER}_{\text{preFEC}}$ ) and output ( $\text{BER}_{\text{postFEC}}$ ) error probability for linear block codes, which for RS (255, 239) can be expressed as

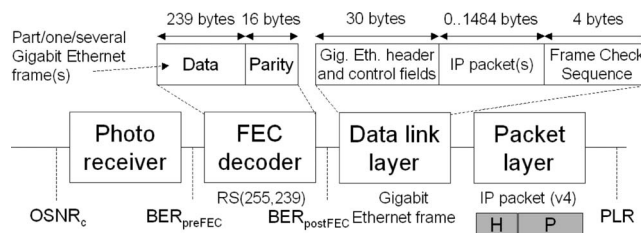


Fig. 2. Receiver side for IP over GigE over WDM with FEC.

$$\begin{aligned} \text{BER}_{\text{postFEC}} = & \frac{17}{255} \sum_{i=9}^{17} \binom{255}{i} \text{BER}_{\text{preFEC}_i}^i (1 - \text{BER}_{\text{preFEC}_i})^{254} \\ & + \frac{1}{255} \sum_{i=18}^{255} i \binom{255}{i} \text{BER}_{\text{preFEC}_i}^i (1 - \text{BER}_{\text{preFEC}_i})^{255-i}. \end{aligned} \quad (4)$$

The assumptions made in [18] are the same as the ones described in Subsection 3.A. For simplicity, we assume that the number of transmitted bits is a multiple of 2040 bits (255 bytes of each RS code word). For each code word, if the number of errors ( $s$ ) and the number of error corrections or erasures performed ( $r$ ) verify  $2s+r < 2t$ , then the original transmitted code word will always be recovered. Otherwise, the result is either a decoder error or a decode failure. This is contained in Eq. (4).

After the FEC decoding, Ethernet frames are reconstructed. Assuming that a single type of IP packet is transmitted for a given WDM channel (lambda service), each frame carries an average number of IP packets  $N$ , each with a length  $L$  (i.e., the payload of the frame is  $NL$ , where  $NL \leq 1484$  bytes for Ethernet as depicted in Fig. 2). We consider that the errors in the payload of a frame will only cause the affected IP packet(s) to be discarded. This technique, called error-locating code, is useful for networking schemes with a high degree of packet aggregation [15]. In this context a packet will be lost in the following situations:

- Error(s) in the header and/or check sequence of the frame ( $C_f=34$  bytes for Ethernet, as depicted in Fig. 2): the  $N$  packets in the frame are lost.
- Error(s) in the  $L$  bits of an IP packet [Eq. (1)] encapsulated in the frame: only that packet is lost.

Kimsas *et al.* provide a closed expression for the average PLR due to physical impairments with respect to the BER (in this paper,  $\text{BER}_{\text{postFEC}}$ ) for such systems [15]:

$$\text{PLR} = 1 - (1 - \text{BER}_{\text{postFEC}})^{C_f} + \frac{1}{N} \sum_{i=1}^N [1 - (1 - \text{BER}_{\text{postFEC}})^{l_i}], \quad (5)$$

where  $l_i$  is the length of an IP packet labeled  $i$  and  $\sum l_i = NL$ . The assumptions made in [15] are the same as the ones described in Subsection 3.A.

## 4. Numerical Results and Discussion

In this section I discuss the numerical results obtained from the expressions derived previously and show the graphical representation of the relation between the PLR and the OSNR.

### 4.A. Service Model

Since optical network technologies are an emerging field, no SLAs have been defined that are adapted to the specific needs of all-optical networks. To the best of my knowledge, only [19] proposes an SLA applied to the optical domain (O-SLA), which considers premium, gold, silver, and bronze services with PLR thresholds of  $10^{-9}$ ,  $10^{-6}$ ,  $10^{-4}$ , and  $10^{-2}$ , respectively.

We assume that a client of the all-optical network is an aggregating device (e.g., an IP router) that aggregates a given traffic type per wavelength, and hence the optical network provides lambda services. We consider that the IP services carried over the network fall within the scope of the triple-play context, i.e., voice over IP (VoIP), video [IP television (IPTV)], and data over IP (Internet). Table 3 summarizes average packet length for each service ( $L$ ), the maximum number of IP packets per GigE frame ( $N_{\text{max}}$ ) and the resulting Ethernet frame length. Due to the variability of Internet data, we consider short and long data packets for Internet data. RS code words are formed with groups of 239 bytes of the Ethernet transmission, which is formed by frames separated with interframe gaps.

In general, IP quality values for triple-play services depend on codec types, bit rates, and concealment algorithms (or buffers). For this reason, in the literature we may find varying PLR values for VoIP, IPTV, and data over IP (Internet). The ITU-T

**Table 3. Characteristics of IP Packets Framed with GigE (in Bits)**

Service	Average Packet Length ( $L$ )	Maximum Number of Packets per Frame ( $N_{\max}$ )	Frame Length
IPTV	1200	9	1384
VoIP	1504	7	1350
Internet (1)	240	49	1504
Internet (2)	11872	1	1518

**Table 4. PLR Thresholds for Triple-Play Services**

Service	Maximum PLR
IP television (IPTV)	$10^{-4}$
Voice over IP (VoIP)	$10^{-3}$
Internet data (1)	$10^{-2}$
Internet data (2)	$10^{-2}$

recommendation Y.1541 [20] defines six network QoS classes based on IP applications: from 0 (most demanding) to 5 (best effort). For classes 0 to 4, this recommendation defines an IP PLR of  $10^{-3}$  (upper bound). Class 5 remains unspecified. As for VoIP, PLR values range from 0% to 5% depending on whether the service is conversational voice, voice messaging, or high-quality audio streaming, and also on the capabilities of the network's higher layers. In this work, I consider the PLR value in Y.1541 for VoIP. Similarly, the PLR for high-quality video streaming ranges from  $10^{-4}$  to  $10^{-7}$  or even less [21].

Another interesting aspect to take into account is that the PLR is usually measured between user interfaces. This means that the PLR measured at the egress of an all-optical network is a factor  $\alpha$  of the PLR specified in the SLA. For this reason, in [15] the authors consider that  $\alpha=0.1$ . For simplicity, and because  $\alpha$  depends on the network size and topology, on the light path and on the upper layers in the OSI stack, in this work we consider  $\alpha=1$ . Table 4 summarizes the PLR values considered for triple-play services carried over a generic all-optical, wavelength-routed network.

#### 4.B. Relation between the OSNR and the BER

Figure 3 illustrates the nonintrusive monitoring scheme considered in this work, which was derived in previous work by the author [13]. The OSNR monitor element in the figure is a spectral monitoring device that taps a small percentage of each fiber and measures the optical power, OSNR, and frequency drift for each active optical channel. The PLR monitor element measures the PLR of the received data after the FEC decoding and Ethernet deframing. We consider GigE and 10GigE as framing for the transport of IP services over the all-optical network. For GigE, we assume  $B_o=12.5$  GHz and  $B_e=12.5$  GHz, whereas for 10GigE we assume  $B_o=12.5$  GHz and  $B_e=2.5$  GHz (Fig. 1).

Figure 4 illustrates the relation of the OSNR at the optical receiver and the estimated BER at the input of the FEC decoder ( $BER_{\text{preFEC}}$ ) according to Eq. (3) as well as the relation between the input and output BER of the FEC decoder ( $BER_{\text{preFEC}}$  and

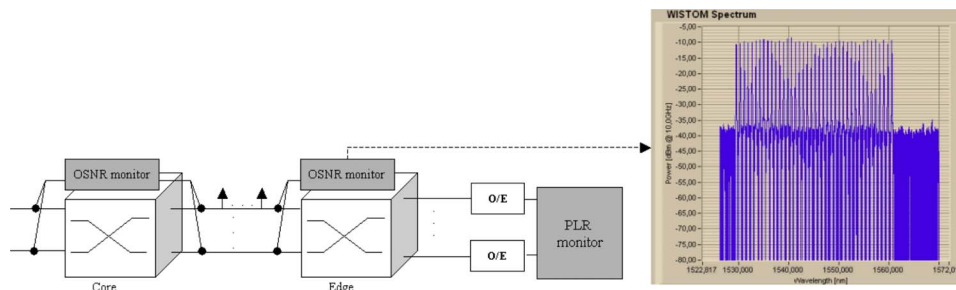


Fig. 3. Monitoring scheme for OSNR and PLR measurement.

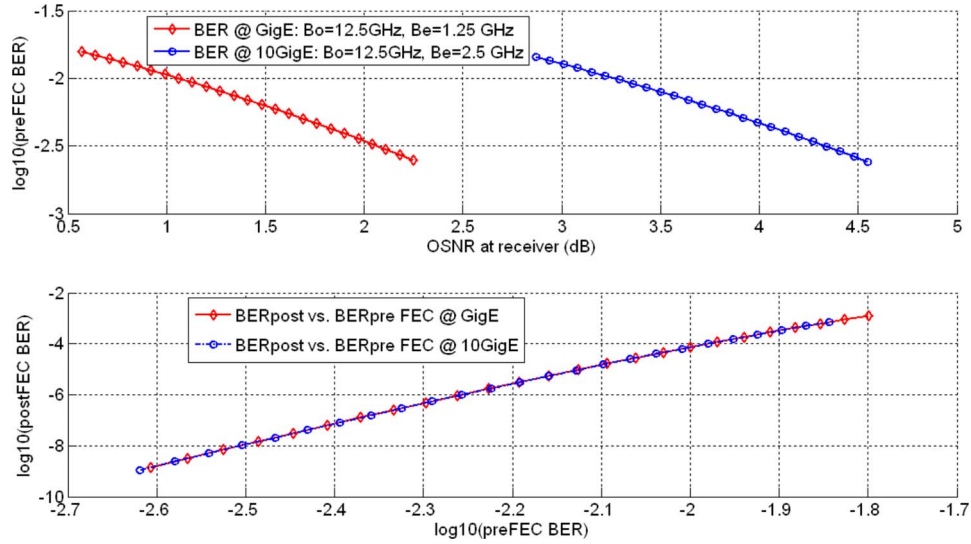


Fig. 4. BER as a function of (top) OSNR and (bottom) input-output FEC.

$BER_{postFEC}$  according to Eq. (4). I plot ranges of OSNR measured at the receiver that lead to errors due to physical impairments (low OSNR). Note that, as expected, the FEC improves the BER significantly [15] and allows really low OSNR margins for the target PLR thresholds (Table 4).

#### 4.C. Relation between the OSNR and the PLR

Now we apply Eq. (5) to the packet and frame size values of Table 3, using the OSNR ranges of Fig. 4 (top). Figures 5-7 plot the relation between the OSNR measured at the photoreceiver and the PLR measured at the client IP router. In all the figures, the maximum target PLR is shown according to the values in Table 4 for GigE and 10GigE transmission.

As demonstrated in [15], the number of IP packets in the Ethernet payload ( $N$ ) does not have an impact on the PLR computed when FEC and error-locating codes are combined. Therefore, the values in Figs. 5-7 use the maximum  $N$  possible for each service (IPTV, VoIP, and Internet data), which is listed in Table 3 ( $N_{max}$ ). For the same OSNR measured at the photoreceiver, different PLR values are measured depending on the parameters  $L$  and  $N$ . We may observe that IPTV and VoIP services are very similar because their  $L$  and  $N$  values are similar (see Table 3). However, the maximum allowed PLR for the IPTV service is  $10^{-4}$ , whereas for VoIP it is an order of magnitude

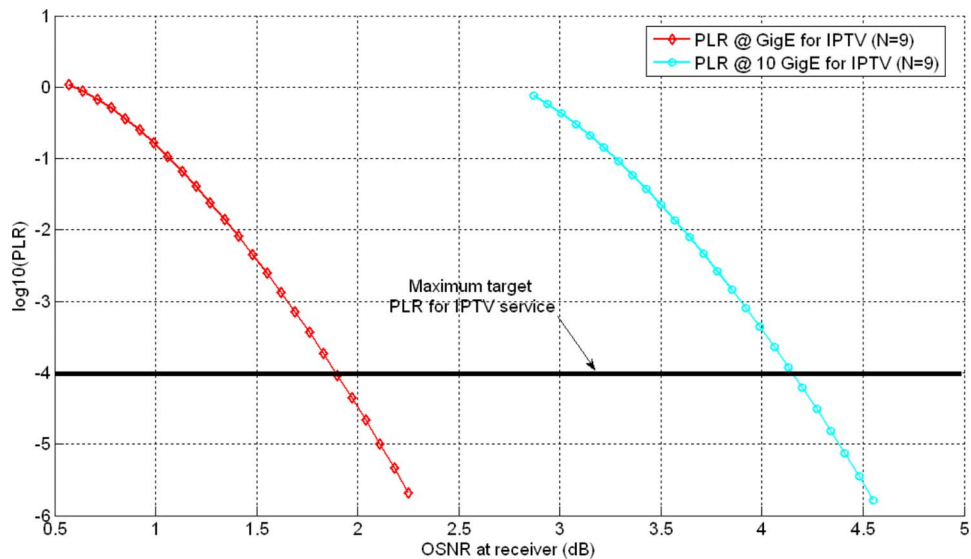


Fig. 5. PLR as a function of OSNR for IPTV service.

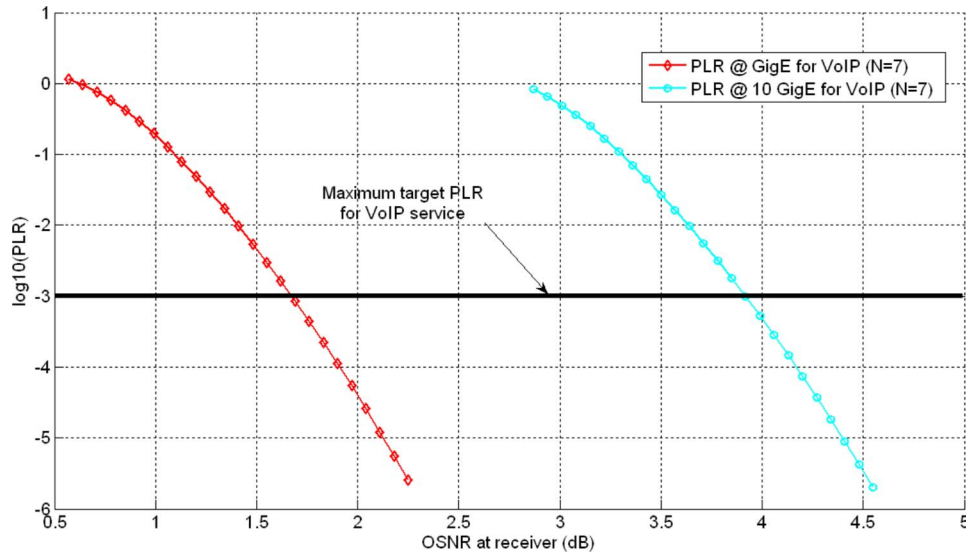


Fig. 6. PLR as a function of OSNR for VoIP service.

lower ( $10^{-3}$ ). Hence, for the same light-path characteristics and FEC scheme, the IPTV service requires at least 1.8 dB OSNR at the receiver for GigE and  $\sim 4.2$  dB OSNR for 10GigE, whereas the VoIP service can ensure sufficient QoS with 0.25 dB less.

This slight difference is much clearer for the Internet service, where short IP packets (240 bits) and long IP packets (11,872 bits) are taken into account for the same PLR threshold ( $10^{-2}$ ; see Table 4). Figure 7 illustrates the relation between the PLR and the OSNR for the Internet service considered in this work. For short data packets, the target PLR is achieved for OSNR margins above 1.3 dB for GigE and 3.5 dB for 10GigE, whereas for long data packets, an extra margin of  $\sim 0.3$  dB is needed for the same PLR value.

Through Eqs. (3)–(5) we are able to relate a measured OSNR value to the equivalent PLR. This OSNR measurement is done at the egress of the light path, right before the photodetector and the FEC decoder (Fig. 2). At this point, this relation can serve different purposes:

- Estimating of the PLR for the OSNR margin at the receiver faster than the IP router, hence helping achieve faster fault detection;

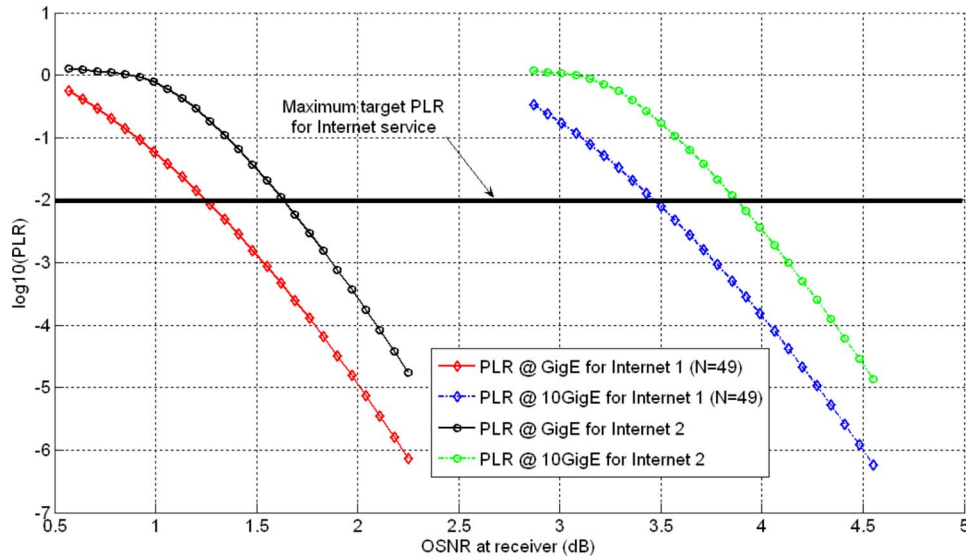


Fig. 7. VoIP PLR as a function of OSNR for Internet data services.

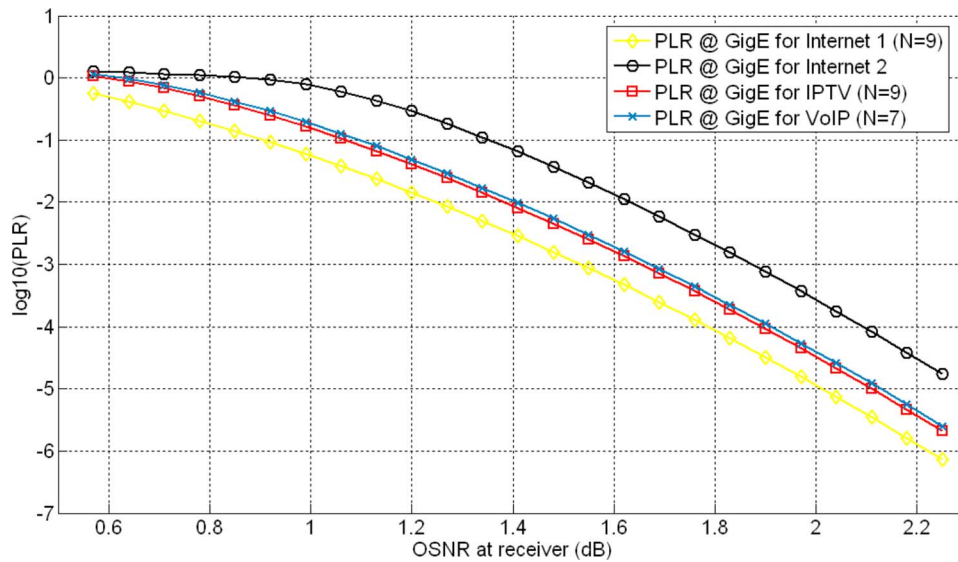


Fig. 8. PLR for triple-play services as a function of OSNR for 1 GigE transmission.

- Relating OSNR variations to PLR decreases, hence helping achieve proactive monitoring and preventive reliability mechanisms;
- Complementing PLR calculations by the IP router, and even avoiding probe IP traffic for PLR estimation.

If the OSNR is measured in the core nodes of the optical network, the analytical relation between the OSNR and the PLR derived in this work has a slightly different purpose, which is more preventive than the previous cases considered. That is, if we are able to relate an OSNR decrease at an intermediate node with a PLR value, we can enhance proactive fault monitoring and minimize data loss in the probable event of a failure (after significant OSNR decrease).

## 5. Conclusions and Future Work

This paper provides an analytical relation of OSNR and PLR that allows combined analog and digital monitoring for SLA guarantee and fault detection. Results in the framework of a FEC-enabled IP-GigE-WDM network have been shown and discussed. These results, which are summarized in Fig. 8 for 1GigE transmission, consist of the derivation of minimum performance thresholds for triple-play services. Future work involves measuring the OSNR and PLR in a real all-optical network [13] to compare the analytical OSNR-PLR relation derived in this paper to the experimental measurement of these performance parameters. This will allow the experimental verification of the analytical relation derived in this work as well as the empirical assessment of some open questions, e.g., whether physical-layer coding has an impact on the BER [22].

## Acknowledgments

This work was partially funded by the Spanish Ministry of Science and Education through the project RESPLANDOR under contract TEC2006-12910/TCM.

## References

1. "Network node interface for the synchronous digital hierarchy (SDH)," ITU-T Recommendation G.707 (ITU, 1996).
2. Y. Kobayashi, Y. Sato, K. Aida, K. Hagimoto, and K. Nakagawa, "SDH-based 10 Gbit/s optical transmission system," in *Proceedings of Global Telecommunications Conference (IEEE, 1994)*, Vol. 2, pp. 1166-1170.
3. Y. Kobayashi, Y. Tada, S. Matsuoka, N. Hirayama, and K. Hagimoto, "Supervisory systems for all-optical network transmission system," in *Proceedings of the Global Telecommunications Conference (IEEE, 1996)*, Vol. 2, pp. 933-937.

4. N. S. V. Rao, "Computational complexity issues in operative diagnosis of graph-based systems," *IEEE Trans. Comput.* **42**, 447–457 (1993).
5. S. Stanic, S. Subramaniam, H. Choi, G. Sahin, and H.-A. Choi, "Efficient alarm management in optical networks," in *Proceedings of the DARPA Information Survivability Conference and Exposition* (IEEE, 2003), Vol. 1, pp. 252–260.
6. P. Nayek, S. Pal, B. Choudhury, A. Mukherjee, D. Saha, and M. Nasipuri, "Optimal monitor placement scheme for single fault detection in optical network," in *Proceedings of the 7th International Conference on Transparent Networks* (IEEE, 2005), Vol. 1, pp. 433–436.
7. C. Mas, I. Tomkos, and O. K. Tonguz, "Failure location algorithm for transparent optical networks," *IEEE J. Sel. Areas Commun.* **23**, 1508–1519 (2005).
8. A. T. Bouloutas, S. Calo, and A. Finkel, "Alarm correlation and fault identification in communication networks," *IEEE Trans. Commun.* **42**, 523–533 (1994).
9. Y. Wen, V. W. S. Chan, and L. Zheng, "Efficient fault-diagnosis algorithms for all-optical WDM networks with probabilistic link failures," *J. Lightwave Technol.* **23**, 3358–3371 (2005).
10. H. Zeng, C. Huang, and A. Vukovic, "A novel fault detection and localization scheme for mesh all-optical networks based on monitoring-cycles," *Photonic Network Commun.* **11**, 277–286 (2006).
11. "Link management protocol (LMP)," IETF RFC 4204 (Internet Engineering Task Force, 2005).
12. H. Zeng, A. Vukovic, and C. Huang, "A novel end-to-end fault detection and localization protocol for wavelength-routed WDM networks," *Proc. SPIE* **5970**, 59702D (2005).
13. C. Pinart, "Alternatives for in-service BER estimation in all-optical networks: towards minimum intrusion," *J. Comput.* **2**, 56–63 (2007).
14. D. A. Schupke, "Broadband Internet access using gigabit Ethernet over wavelength-division multiplexing (WDM) networks," in *Fifth EUNICE Open European Summer School* (EUNICE Network, 1999).
15. A. Kimsas, H. Øverby, S. Bjørnstad, and V. L. Tuft, "A cross layer study of packet loss in all-optical networks," in *Proceedings of the Advanced International Conference on Telecommunications and International Conference on Internet and Web Applications and Services (AICT/ICIW)* (IEEE, 2006), pp. 65–71.
16. P. A. Humblet and M. Azizoglu, "On the bit error rate of lightwave systems with optical amplifiers," *J. Lightwave Technol.* **9**, 1576–1582 (1991).
17. D. Marcuse, "Derivation of analytical expressions for the bit-error probability in lightwave systems with optical amplifiers," *J. Lightwave Technol.* **8**, 1816–1823 (1990).
18. D. J. Torrieri, "The information bit error rate for block code," *IEEE Trans. Commun.* **COM-32**, 474–476 (1984).
19. W. Fawaz, B. Daheb, O. Audouin, M. Du-Pond, and G. Pujolle, "Service level agreement and provisioning in optical networks," *IEEE Commun. Mag.* **42**, 36–43 (2004).
20. "Network performance objectives for IP-based services," ITU-T Recommendation Y.1541 (ITU, 2006).
21. K. Kerpez, D. Waring, G. Lapiotis, J. Lyles, and R. Vaidyanathan, "IPTV service assurance," *IEEE Commun. Mag.* **44**, 166–172 (2006).
22. A. W. Moore, L. B. James, M. Glick, A. Wonfor, R. G. Plumb, I. H. White, D. McAuley, and R. V. Penty, "Optical network packet error rate due to physical layer coding," *J. Lightwave Technol.* **23**, 3056–3065 (2005).